FIZIKA Volume 21, Supplement 1, 1989.
Proceedings of the XI Yugoslav SYMPOSIUM OF THE PHYSICS OF CONDENSED MATTER.
M. Davidović and M. Lj. Napijalo Editors, Donji Milanovac, October 3–7, 1988.

MAGNETIC STRUCTURES OF RARE EARTH COMPOUNDS

Andrzej Szytuła

Institute of Physics, Jagellonian University, Kraków, Poland

In review magnetic structures of two groups of rare earth compounds i.e. intermetallics of RT_2X_2-type and high T_c-superconductors are discussed. In RT_2X_2 compounds a number of different magnetic ordering types of the rare earth sublattice is observed. The transition metal sublattice orders only in the case of Mn. In high T_c-superconductors magnetic moments of Cu atoms order magnetically at high temperatures and an antiferromagnetic ordering in rare earth sublattices is observed at low temperatures. For both groups of compounds the observed magnetic structures are discussed in terms of exchange interactions and crystalline fields effects.

1. INTRODUCTION

Relation between magnetism and superconductivity has been a matter of considerable interest for many years. In ternary magnetic superconductors such as $ErRh_4B_4$ and $HoMo_6S_8$ magnetic and superconducting electrons occupy separate sublattices. Hence there is only a weak coupling between those two cooperative effects /1/.

In this review properties connected with magnetism and superconductivity in two groups of rare earth compounds, namely intermetallics of RT_2X_2 type /R- rare earth, T - transition metal, X=Si, Ge/ and high T_c superconductors: $La_{2-x}T_xCuO_4$ /T=Ba,Sr/ and $RBa_2Cu_3O_{7-x}$, are reported. In both groups of compounds the rare earth atoms and the transition metal ones occupy two different crystal sites.

2. INTERMETALLIC RT_2X_2 COMPOUNDS

During recent years, intermetallic compounds prepared on the basis of 4f-electron elements have been a subject for intensive studies because of their intriguing physical properties. Among the in compounds of general formula RT_2X_2 are particularly numerous and interesting.

Most of RT_2X_2 compounds crystallize in the body-centered tetragonal structure of $ThCr_2Si_2$-type /space group I4/mmm/ /2/. This type of crystal structure consists of tetrahedra build up of X atoms with a transition metal inside. Its atomic framework can be alternatively visualised as the following sequence of monoatomic planes:

R - X - T - X - R - X - T - X - R.

The unit cell of $ThCr_2Si_2$ type is shown in Fig. 1.

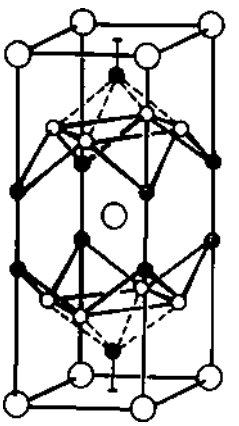

Fig. 1

According to the authors best knowledge, magnetic properties, including magnetic structure of more than 100 rare earth compounds of the $ThCr_2Si_2$ type structure have been examined. Magnetic data concerning these compounds are collected in /3/.

Neutron diffraction data indicate that the rare earth sublattices exhibit a large variety of ordering schemes /see Fig. 2/:

1. collinear ferromagnetism /F/ was found in $TbMn_2X_2$ and $ErMn_2X_2$ /X=Si,Ge/,
2. four types of collinear antiferromagnetic structures:
   - type AFI with the wave vector $\vec{k}$=/0,0,1/ was observed in RCo_2X_2 /R=Pr-Tm/, RRh_2Si_2 and RRh_2Ge_2 /R=Nd-Tm/, $TbIr_2Si_2$, $PrCu_2X_2$ and $CeAu_2Si_2$,
   - type AFII with $\vec{k}$=/0,0,$\frac{1}{2}$/ was found in $NdFe_2Si_2$, $NdFe_2Ge_2$, $PrFe_2Ge_2$ and $ErFe_2Si_2$,
   - type AFIII described by $\vec{k}$=/$\frac{1}{2}$,$\frac{1}{2}$,0/ is adopted by $TbNi_2Si_2$, $CeRh_2Si_2$ and $CePd_2Si_2$,

- type AFIV with $\vec{k}=/\frac{1}{2},0\frac{1}{2}/$ is exhibited by RCu_2X_2 /R=Tb-Er/.

3. a number of different non-collinear structures was also discovered:
   - cosinusoidally modulated longitudinal spin wave LSW I propagating along the c-axis was found in $PrCo_2Ge_2$, $HoNi_2Ge_2$ and $PrNi_2Si_2$,
   - cosinusoidally modulated longitudinal spin wave LSW II propagating along the a axis operates in RRu_2Si_2 /R=Tb-Er/, $TbRu_2Ge_2$, ROs_2Si_2 /R=Tb,Ho,Er/ and $CeAg_2Si_2$. In the case of $TbRu_2Si_2$ and $TbRu_2Ge_2$ at low temperatures this type of magnetic structure transforms to the square modulated phase.

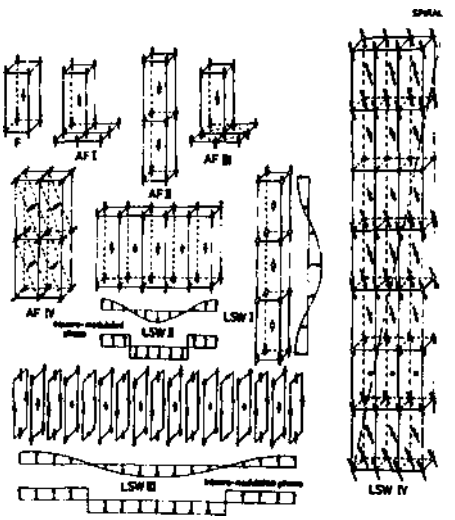

Fig. 2

   - $NdRu_2Si_2$ and $NdRu_2Ge_2$ have complex magnetic structures. Below T=10 K they are ferromagnetic with the moments parallel to c-axis. Above T=10 K $NdRu_2Si_2$ has a cosinusoidally modulated longitudinal spin wave, LSW III propagating along the [111] direction. A squaring of the magnetic structure is observed below T=15 K,
   - LSW IV is incommensurate structure with two component wave vectors $\vec{k}=/k_x,0,k_z/$ occurs in $TbFe_2Si_2$, $HoFe_2Si_2$, $TbPd_2Si_2$, $HoPd_2Si_2$ and $TbPd_2Ge_2$.

Since the interatomic distances between two R atoms are always about 0.4 nm in the basal plane and about 0.6 nm along c-axis, the assumption of the Heisenberg type interaction is not justified. The models involving indirect coupling are usually adopted to

explain the stability of particular magnetic structures.

Since the 4f electrons are strongly localized and the RT_2X_2 systems show a metallic type of electric conductivity, the exchange interactions of 4f electrons can be described in terms of the well-known RKKY theory /4/, which postulates the coupling between the moments via conduction electrons. The other factors are the interaction of the f-electron shells with the crystal field CEF and the interactions with valence electrons of the anionic lattice via hybridization orbitals.

The competition of these factors causes that a large variety of magnetic structures in RT_2X_2 systems occurs. To estimate, which of them plays more important role in the particular compound a plot of the observed Néel temperatures against the de Gennes factor $/g-1/^2 J/J+1/$ has been constructed. The following condusions can be drawn:

- de Gennes function is not obeyed in RT_2X_2 compounds containing light rare earth atoms. In many cases the compounds remain paramagnetic above the temperatures of 1.8 K,
- in the case of heavy rare earth atoms, Néel points follow in principle the de Gennes function.

In an isotropic RKKY model with a spherical Fermi surface, the Fermi vector is strongly dependent on the $\frac{c}{a}$ ratio and on the number of free electrons Z per magnetic ion: $k_F = (2\pi/a)\sqrt[3]{6Za/\pi c}$.

The analysis of c/a values determined for a large number of RT_2X_2 compounds containing heavy rare earth atoms /R=Tb-Tm/ shows, that when $a/c < 0.415$, a simple collinear antiferromagnetic ordering is observed, while the compounds with $a/c > 0.415$ exhibit oscillatory magnetic structures. The stability of observed magnetic structures for Z values near 3. The Z and $\vec{k}$ values obtained up to now for a number of RT_2X_2 compounds are listed in Table 1.

The Interaction of crystalline electric fields /CEF/ with the multiple moments of R atom electrons in a site of a crystal lattice of 4/mmm point symmetry is given by the Hamiltonian

$$H_{CF} = B_2^0 O_2^0 + B_4^0 O_4^0 + B_4^4 O_4^4 + B_6^0 O_6^0 + B_6^4 O_6^4$$

Table 1. The values of k and Z obtained for RT_2X_2 compounds

Compound	$\vec{k}$	Z	Compound	$\vec{k}$	Z
$TbRu_2Si_2$	$0.233\vec{a}^*$	3.13	RCo_2X_2	$1.0\vec{c}^*$	2.75-3.75
$DyRu_2Si_2$	$0.22\vec{a}^*$	3.136	RRh_2Si_2	$1.0\vec{c}^*$	2.77-3.39
/Ho,Er/Ru_2Si_2	$0.2\vec{a}^*$	3.16	$TbRh_2Ge_2$	$1.0\vec{c}^*$	2.84-3.2
$TbRu_2Ge_2$	$0.235\vec{a}^*$	3.0	$NdRu_2Si_2$	$0.0\vec{c}^*$	2.67-3.4
$TbOs_2Si_2$	$0.312\vec{a}^*$	3.0			
/Ho,Er/Os_2Si_2	$0.295\vec{a}^*$	3.02			

Table 2. The values of B_2^0 coefficients and direction of magnetic moment for RT_2Si_2 compounds

R/T	Mn	Fe	Co	Ni	Cu	Rh
Ce					-3.0	$\perp c$
Pr	-0.7,$\parallel c$		$\parallel c$	-3.99,$\parallel c$	$\parallel c$	
Nd		-0,63,$\parallel c$	$\parallel c$	$\perp c$	+0.8,$\perp c$	$\parallel c$
Tb	$\parallel c$	-3.0, $\parallel c$	$\parallel c$	$\parallel c$	+0.57,$\perp c$	-2.4,$\parallel c$
Dy	-1.35	-1.8	-1.0,$\parallel c$	+0.17	+0.175,$\perp c$	-0.22,φ
Ho		-0.61, φ	$\parallel c$	$\perp c$	-0.2	φ
Er	c	+0.67,$\perp c$	$\perp c$	$\perp c$	-0.79,$\parallel c$	$\perp c$
Tm		+2.54	$\perp c$	$\perp c$		$\perp c$
Yb		+7.65,$\perp c$	$\perp c$			

where O_n^m is the Stevens operator, B_n^m is a CEF parameter defined by Hutchings /5/. The c-axis of the tetragonal unit cell was chosen as a quantization axis.

The orientation of the magnetic moment in respect to the tetragonal axis can be connected with the sign of the B_2^0 coefficient. It was shown /6/ that when the magnetic moment is normal to the tetragonal axis or makes an angle φ with it, B_2^0 is positive. For a negative value of B_2^0 coefficient the magnetic moment is parallel to the c-axis. Table 2 contains the values of B_2^0 coefficients determined for a number of RT_2X_2 compounds. These data indicate that the

correlation between the signs of the B_2^0 coefficient and the orientation of magnetic moments agrees with that deduced from neutron diffraction experiments. However, it has been shown, that the sign of B_2^0 depends also on the number of 4f and nd electrons, but the lack of data does not permit us to plot a detailed diagram.

In this section we concentrate on superconducting properties of RT_2X_2 compounds. The list of the compounds is given in Table 3. Superconductivity is observed at very low temperatures and only for nonmagnetic compounds with R=Y,La,Lu and T=Ni,Cu,Rh,Ir,Pd,Pt.

Temperature dependence of the specific heat indicates that $CeCu_2Si_2$ is a superconductor below ~0.5 K. The electronic specific heat constant γ=1.1 J/mol.K^2 suggests that $CeCu_2Si_2$ is a heavy-fermion system /with an effective mass ~100 m_0/ /7/.

Table 3. Superconductivity of RT_2X_2 compounds /7-10/

Compound	T_c/K/	Compound	T_c/K/	Compound	T_c/K/
YPd_2Si_2	0.47	$LaPd_2Si_2$	0.39	$LuPd_2Si_2$	0.67
YRh_2Si_2	0.33	$LaRh_2Si_2$	0.074	$LuRh_2Si_2$	0.33
YIr_2Si_2	2.83	$LaIr_2Si_2$	1.58	$YbPd_2Ge_2$	1.17
YPt_2Si_2	1.70	$LaPt_2Si_2$	1.42	$CeCu_2Si_2$	0.5
		$LaPd_2Ge_2$	1.12		
		$LaPt_2Ge_2$	0.55		
		$LaNi_2Ge_2$	0.69		

3. HIGH-T_c SUPERCONDUCTIVITY

Less than three years ago K.A. Miller and J.G. Bednorz /11/ discovered a material that was superconducting at relatively high temperature /~30 K/. In the second step they have determined the new class of superconductors, $RBa_2Cu_3O_{7-x}$ with high critical temperature i.e. above the boiling point of liquid nitrogen /12/.

Measurements of magnetic susceptibility and resistivity of $RBa_2Cu_3O_{7-x}$ samples indicate transition into a superconducting

state at about 90 K. Specific heat measurements carried out for $RBa_2Cu_3O_7$ /R=Gd,Dy,Ho,Er/ indicate anomalies at 2.24 K, 0.96 K, 0.17 K and 0.59 K for R=Gd, Dy, Ho and Er, respectively /13/. In the case of $GdBa_2Cu_3O_6$ such an anomaly corresponding to a phase transition into an antiferromagnetic state is observed at T_N=2.2 K. Neutron diffraction data collected at T=1.3 K for $GdBa_2Cu_3O_7$ indicate magnetic ordering with doubling of the orthorhombic unit cell in all three dimensions which corresponds with antiferromagnetic ordering. Analysis of the intensities of the observed magnetic Bragg reflections shows that in the ordered state the value of the magnetic moment per Gd atom is $7.4\pm0.6\ \mu_B$ and the moment is parallel to the c-axis of the orthorhombic unit cell. /14/. For $GdBa_2Cu_3O_6$ the magnetic ordering is described by the wave vector $\vec{k}=/\frac{1}{2},\frac{1}{2},0/$. In contrast to the case of $GdBa_2Cu_3O_7$, the magnetic moments of Gd in $GdBa_2Cu_3O_6$ are coupled antiferromagnetically in the a-b plane but ferromagnetically along the crystallographic c-axis./15/.

For $ErBa_2Cu_3O_7$, specific heat measurement indicate the Néel temperature T_N=0.59 K. Below T_N, two-dimensional magnetic ordering with ferromagnetic coupling along b-axis and antiferromagnetic one along a-axis is observed /16/. The neutron diffraction pattern obtained at T=140 mK shows clearly three-dimensional ordering of the Er moments at this temperature. The magnetic reflections can be indexed using two independent wave vectors: $\vec{k}_1=/\frac{1}{2},0,0/$ and $\vec{k}_2=/\frac{1}{2},0,\frac{1}{2}/$. The likeliest model is the one with all moments make an angle of 32 deg. with the crystallographic c-axis. The value of the ordered magnetic moment at T=140 mK is $4.9/2/\ \mu_B$ which is much less than the free-ion value of Er^{3+} /17/.

Below the Néel point T_N=0.90/3/ K, neutron diffraction studies of $DyBa_2Cu_3O_{6.95}$ indicate three-dimensional long-range antiferromagnetic similar to the S-state of $GdBa_2Cu_3O_7$. This magnetic structure is characterized by the vector $\vec{k}=/\frac{1}{2},\frac{1}{2},\frac{1}{2}/$ and the magnetic moments of Dy^{3+} are parallel to the c-axis and saturated to $6.8/1/\ \mu_B$ /18/. The magnetic structure of $DyBa_2Cu_3O_7$ is presented in Fig. 3.

In the case of $HoBa_2Cu_3O_{6.8}$ a broad peak presumably magnetic

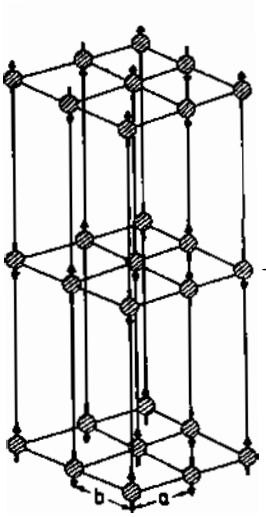

Fig. 3

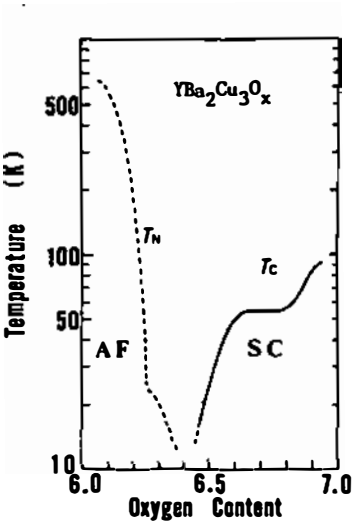

Fig. 4

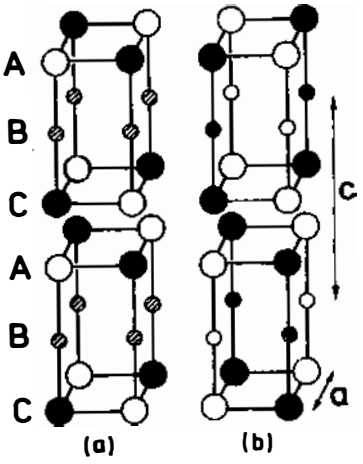

Fig. 5

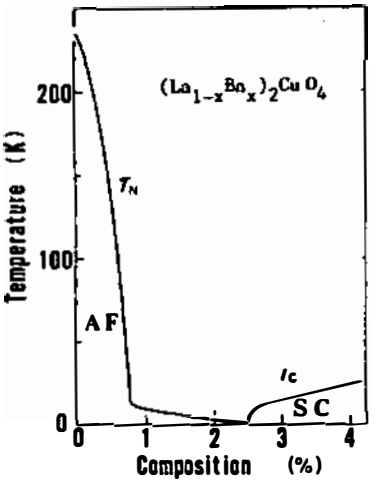

Fig. 6

origin appears below T_N=140/15/ mK. This is in good agreement with earlier heat capacity measurement /13/. The peak appears at the similar position as it was found for the 2D-antiferromagnet $ErBa_2Cu_3O_7$ /16/, but its shape is considerably less asymetric. This indicate short range range antiferromagnetic correlations between ordered planes /19/.

What is the nature of interactions which produce antiferromagnetic ordering of the rare earth sublattice in rare earth based superconductors?

Trying to answer this question we can select three main mechanisms:

1. exchange interactions between localized 4f moments via conduction electrons. Values of Néel temperatures does not satisfy the de Genmes function - large discrepances are observed for Ho and Er. This suggests that some different mechanisms of interaction are decisive in developing the magnetic structure of the $RBa_2Cu_3O_7$ systems.
2. dipole-dipole interactions. Calculations of the dipole energy for the observed magnetic structure of $GdBa_2Cu_3O_7$ show that the energy required to flip one Gd moment is 1.40 K.
3. interaction through anions. The observed magnetic structures of $GdBa_2Cu_3O_7$ and $GdBa_2Cu_3O_6$ indicate significant influence of oxygen occupancy on magnetic ordering.

The reduction of magnetic moment in the ordered state of Er- and Dy- based compounds is clear evidence for importance of crystal field effects in these compounds.

Crystal structure and physical properties of $YBa_2Cu_3O_{7-x}$ strongly depend on the oxygen content of the compound /20/. The magnetic and superconducting phase diagram is presented in Fig. 4 /21/. The oxygen content in this compound can easily be varied from 7 to 6. With increasing oxygen deficiency x, the superconducting T_c decreases and for low content of oxygen antiferromagnetic ordering is observed. Neutron diffraction experiments shows that $YBa_2Cu_3O_6$ orders antiferromagnetically below T_N=420±10 K. The magnetic moment of 0.60/5/ μ_B is

localized on Cu^{2+} sites and is perpendicular to the tetragonal c-axis. The magnetic structure is characterized by the in-plane wave vector $/\frac{1}{2},\frac{1}{2},0/$ and the antiferromagnetic coupling between CuO_2 planes in the unit cell. An increase in the oxygen contents leads only to, a decrease in T_N and in the magnetic moment value /290/10/ K, 0.45/5/ μ_B and 245/10/ K, 0.28/5/ μ_B for x=0.25/3/ and 0.38/3/, respectively. The long range magnetic order disappears abruptly around x=0.4 /22/.

A different type of magnetic structure is determined in $NdBa_2Cu_3O_6$. In this compound magnetic moments are localized on Cu/2/ ions and order antiferromagnetically at T_{N1}=450 K. Below T_{N2}=80 K the observed magnetic structure is described by the wave vector $/\frac{1}{2},\frac{1}{2},\frac{1}{2}/$. Very small magnetic moment of 0.12 μ_B is observed on Cu/1/ chain atoms /see Fig. 5/ /23/.

The schematic phase diagram of $/La_{1-x}Ba_x/_2CuO_4$ is shown in Fig. 6 /21/. The stoichiometric compound La_2CuO_4 exhibit antiferromagnetic properties /24/. On the increase of Ba contents the value of the Néel temperature decreases and above 0.01 the antiferromagnetic order disappears. New experimental data indicate existence of a new intermediate phase between the antiferromagnetic and the superconducting phases /24/.

The neutron diffraction experiment carried out for La_2CuO_4 indicate antiferromagnetic ordering below ~220 K /25/. From the magnetic peak intensities we deduced the structure consisting of ferromagnetic sheets of Cu spins alternating along the [100] orthorhombic axis, with spins in the planes parallel to the [001] orthorhombic axis. The low temperature magnetic moment is approximately 0.5 μ_B/Cu atom.

Magnetic properties of this compound strongly depend on oxygen vacancies created by heat treatment. In Table 4 the values of the Néel temperatures and the magnetic moment, determined by us and by other authors, are collected.

In both $YBa_2Cu_3O_6$ and La_2CuO_4 compopounds, high values of the ordering temperature proves strong magnetic coupling. The crystal

structure and the type of magnetic ordering exhibit a pronounced two-dimensional character. The magnetic interactions are described by two exchange integrals: J /in plane/ and J' /interplanar/. The quasi two-dimensional character of magnetic ordering suggests the relation $J' \ll J$. Interpretation of these exchange interactions is difficult because one has to deal with complicated crystal structure and unknown nature of magnetic interaction mechanisms.

Thus, summarizing the phenomenon of coexistence of superconductivity and magnetism in rare-earth compounds is very rare. The coexistence is observed only in these compounds in which magnetic interactions are very weak and lead to antiferromagnetic ordering.

Properties of high T_c superconductors should stimulate intensive experimental and theoretical exploration of coexistence of these two phenomenon.

Table 4. Magnetic properties from different La_2CuO_4 Samples

Sample	T_N/K/	μ/μ_B/	Ref.
powder	220	0.5	25
powder	250	0.40/5/	26
untreated crystal	150	0.23/5/	26
400 °C treated crystal	50	0.17/5/	26
powder	240	0.5/1/	this work

REFERENCES

1. B. Coqblin, J. Magn. Magn. Mat. 29 /1982/ 1.
2. Z. Ban and M. Sikirica, Acta Cryst. 18 /1965/ 594.
3. A. Szytuła and J. Leciejewicz, in Handbook on Physics and Chemistry of Rare Earths, ed. K.A. Gschneider Jr. and L.Eyring, Amsterdam, North-Holland, vol. 12, 1988, in press.
4. M.A. Ruderman and C. Kittel, Phys. Rev. 96 /1954/ 99, K. Yosida, Phys. Rev. 106 /1957/ 893, T. Kasuya, Prog. Theor. Phys. 16 /1956/ 45.

5. N.T. Hutchings, Solid State Phys. 16 /1964/ 227.
6. J.E. Greedan and V.U.S. Rao, J. Solid State Chem. 8 /1973/368.
7. G.R. Stewart, Reviews of Modern Physics, 56 /1984/ 755.
8. R.N. Shelton, H.F. Braun and E. Musick, Solid State Commun. 25 /1984/ 797.
9. T.T. Palstra et al. Phys. Rev. 34B /1986/ 4566.
10. G.W. Hull et al. Phys. Rev. 24B /1981/ 6715.
11. J.G. Bednorz and K.A. Müller, Z. Phys. B64 /1986/ 189.
12. M.K. Wu et al. Phys. Rev. Lett. 58 /1987/ 908.
13. B.D. Dunlap et al. J. Magn. Magn. Mat. 68 /1987/ L139.
14. D. McK. Paul et al. Phys. Rev. B /1988/ in press.
15. T. Chattopadhyay et al., J. de Physique,/1988/ in press.
16. J.W. Lynn et al. Phys. Rev. B36 /1987/ 2374.
17. T. Chattopadhyay et al. J. de Physique /1988/ in press.
18. A.J. Goldmann et al. Phys. Rev. B36 /1987/ 7234.
19. P. Ferrer, private communication.
20. H. Kadowaki et al. Phys. Rev. B37 /1988/ 7932.
21. S. Uchida, Int. J. of Modern Physics B2 /1988/ 181.
22. P. Burlet et al. Physica C153-155 /1988/ 1115.
23. W.H. Li et al. Phys. Rev. B /1988/ in press.
24. P.M. Grant et al. Phys. Rev. Lett. 58 /1987/ 2482.
25. D. Vaknin et al. Phys. Rev. Lett. 58 /1987/ 2802.
26. T. Freltoft et al. Phys. Rev. B36 /1987/.